Simultaneous Stabilization Example

Multiple Bounded Stability Domains and Reconfigurable Control

A. Plant Models and Stability Domains

The two open-loop linear system models are given by Type 1, 2nd-order transfer functions. These transfer functions are:

$$p_0(s) = \frac{\omega_{n0}^2}{s(s+2\zeta_0\omega_{n0})} = \frac{4}{s(s+2)}, \qquad \zeta_0 = 0.5, \quad \omega_{n0} = 2\ r/s \tag{1}$$

$$p_1(s) = \frac{\omega_{n1}^2}{s(s+2\zeta_1\omega_{n1})} = \frac{16}{s(s+0.8)}, \qquad \zeta_1 = 0.1, \quad \omega_{n1} = 4\ r/s \tag{2}$$

Two scenarios will be considered. Scenario A will consider p_0 to be the nominal system and p_1 to be a perturbation. Stability domains will be defined for this condition, and a simultaneously stabilizing compensator will be designed for it. Scenario B will consider p_1 to be the nominal system and p_0 to be a perturbation. Stability domains will be defined for this condition also, and a second simultaneously stabilizing compensator will be designed.

For scenario A, the stability domains are denoted D_{0A} and D_{1A} for systems p_0 and p_1, respectively. Similar notations are used for scenario B. The real axis limits on the four domains are shown in Table 1. The imaginary axis limits are obtained by multiplying the real axis limits by the corresponding value of slope shown in the table. The settling times (T_s) and percent overshoots (PO) in the table are for step responses for the standard second-order system model

$$\frac{Y(s)}{R(s)} = \frac{\omega_n^2}{s^2 + 2\zeta\omega_n s + \omega_n^2} \tag{3}$$

which would be obtained by placing unity feedback around a plant model such as p_0. $Y(s)$ and $R(s)$ are the Laplace transforms of the output and reference input signals, respectively. The values for the settling times and percent overshoots are calculated from the following expressions.

$$T_s = \frac{4}{\zeta\omega_n}, \quad \text{PO} = \left(e^{-\pi\zeta/\sqrt{1-\zeta^2}}\right) \times 100\% \tag{4}$$

Table 1: Definitions of the Stability Domains.

Domain	Real Axis	Settling Time (s)	ζ	Slope	Overshoot (%)
D_{0A}	-1.5 to -5	2.67 to 0.8	0.707	1	4.3
D_{1A}	-0.5 to -6	8 to 0.667	0.4	2.2913	25.4
D_{0B}	-0.25 to -4.5	16 to 0.889	0.4	2.2913	25.4
D_{1B}	-0.5 to -4	8 to 1	0.707	1	4.3

The two plant models represent the same physical system in two different operating conditions. Closed-loop stability is to be guaranteed for both systems. The stability domains are selected to provide good performance as well as stability for the nominal system and allow degraded performance but not loss of stability for the perturbed system. For this example, the stability domains are chosen rather arbitrarily. In general, the right-most real axis limit would be chosen based on settling time specifications, and the value of ζ would be chosen to determine the imaginary axis limits based on maximum overshoot specifications. The left-most real axis limit might be chosen to limit the peak magnitude of the control signal.

These notes are lecture notes prepared by Prof. Guy Beale for presentation in Spring 2004 for ECE 699, *Special Topics in Robust Control: Simultaneous Stabilization*, in the Electrical and Computer Engineering Department, George Mason University, Fairfax, VA. Additional notes can be found at the following website: http://teal.gmu.edu/~gbeale/examples.html.

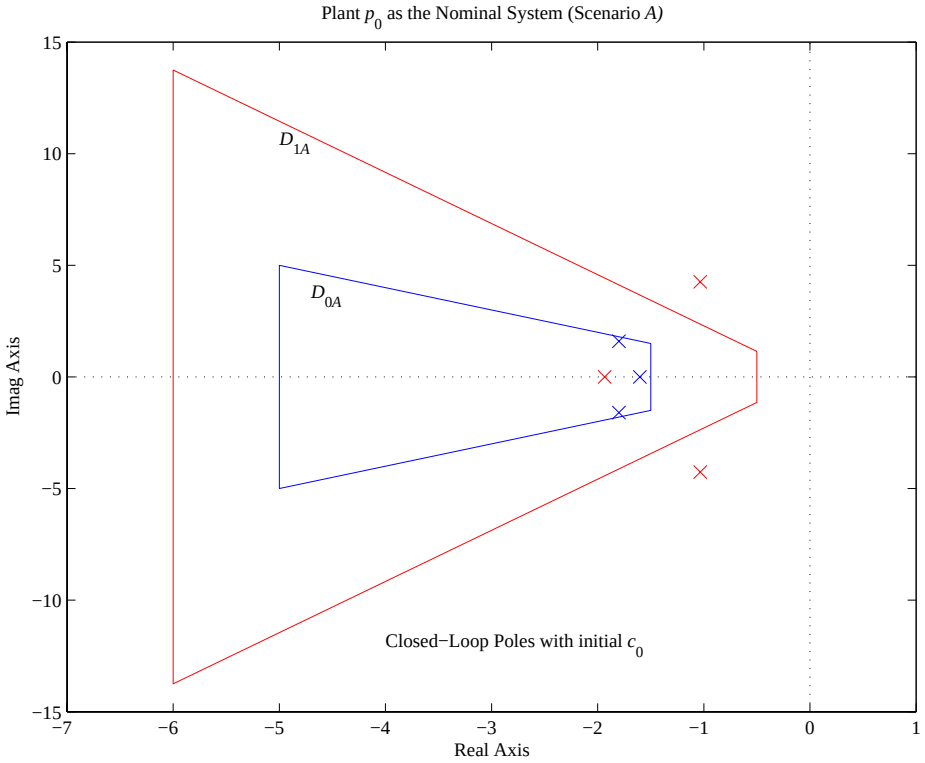

Fig. 1. Closed-loop poles for $\{c_0, p_0\}$ and $\{c_0, p_1\}$ for Scenario A.

B. Initial Design of the Compensators

The starting point will be to design a compensator that will stabilize plant p_0 with respect to domain D_{0A}, which is the domain for p_0 in scenario A. A simple phase lead compensator is designed using root locus techniques[1] to place a dominant closed-loop pole at $s = -1.8 + j1.6$. No restrictions are placed on the structure of the compensator or on the closed-loop stability of plant p_1 with this compensator. The initial compensator for p_0 is

$$c_{0A} = \frac{1.2911\,(s + 1.8)}{(s + 3.2027)} \tag{5}$$

The closed-loop poles for p_0 and p_1 when p_0 is considered the nominal plant are shown in Fig. 1. The closed-loop poles of p_0 are shown in blue, and the closed-loop poles for p_1 are shown in red. It is clear that this compensator does stabilize p_0 with respect to D_{0A}. Plant p_1 is also stabilized, but not entirely with respect to D_{1A}. If p_1 had been stabilized with respect to D_{1A}, then the design process for scenario A would have been completed at this stage.

Before continuing with the design process for scenario A, we will design the initial compensator for plant p_1 which will stabilize it with respect to stability domain D_{1B}, which is the domain for p_1 in scenario B. Again a root locus design method is used to place a dominant closed-loop pole, this time at $s = -0.8 + j0.7$. A compensator that accomplishes this is

$$c_{1B} = \frac{0.1049\,(s + 1)}{(s + 2.2848)} \tag{6}$$

The plots in Fig. 2 of the closed-loop poles for p_1 and p_0 when p_1 is considered the nominal system show that this compensator does stabilize p_1 with respect to D_{1B}. Again, the closed-loop poles of p_0 are shown in blue, and the closed-loop poles for p_1 are shown in red. Plant p_0 is also stabilized, but not entirely with respect to D_{0B}. As before, if p_0 had been stabilized with respect to D_{0B}, then the design process for scenario B would have been completed at this stage.

C. The Controller Design for Scenario A

The remaining design steps for scenario A will now be undertaken. The associated system p_{01A} [1]–[3] will be formed from the coprime factorizations of the original system models and the initial compensator c_{0A}. The factorizations are

[1]See http://teal.gmu.edu/~gbeale/ece_421/examples_421.html

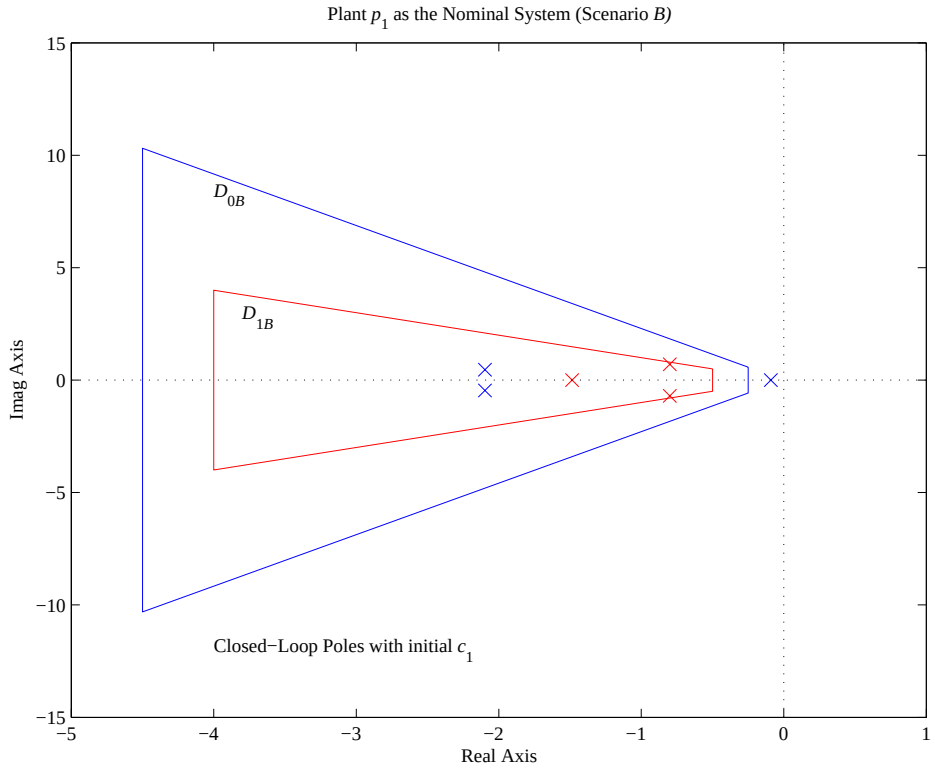

Fig. 2. Closed-loop poles for $\{c_1, p_0\}$ and $\{c_1, p_1\}$ for Scenario B.

$$n_0 = \frac{4}{(s+3)^2}, \quad d_0 = \frac{s(s+2)}{(s+3)^2}, \quad n_1 = \frac{16}{(s+3)^2}, \quad d_1 = \frac{s(s+0.8)}{(s+3)^2} \tag{7}$$

$$x_{0A} = \frac{1.2911(s+1.8)}{(s+3)}, \quad y_{0A} = \frac{(s+2.2027)}{(s+3)} \tag{8}$$

and the associated system is

$$p_{01A} = \frac{(d_0 n_1 - d_1 n_0)}{x_{0A} n_1 + y_{0A} d_1} = \frac{b_{01A}}{a_{01A}} = \frac{12s(s+2.4)}{(s+1.935)(s+3)(s+1.034 \pm j4.26)} \tag{9}$$

As shown in Fig. 3, this associated system satisfies the extended parity interlacing property (e.p.i.p.) [4] with respect to domain D_{1A}, which is a necessary condition for the problem to be solved. The only interval of interest in the extended complement of D_{1A} is between the open-loop zeros at 0 and ∞. There are no open-loop poles in that interval, so e.p.i.p. is satisfied.

In order to simultaneously stabilize p_0 and p_1 with respect to domains D_{0A} and D_{1A}, it is necessary and sufficient that p_{01A} be stabilized with respect to D_{1A} by a compensator that is stable with respect to the intersection of D_{0A} and D_{1A} [4]–[7]. In this example, the area of intersection is D_{0A}. This is termed the Double-D stabilization problem [8]–[11]. One compensator that accomplishes this is

$$r_{0A} = \frac{3.303(s+1.46)^2}{(s+4.28)^2} \in S^{D_{0A}} \tag{10}$$

The closed-loop poles for (r_{0A}, p_{01A}), shown in red in Fig. 4, are seen to lie inside D_{1A}, and the two repeated compensator open-loop poles, shown in blue, are in D_{0A}. Thus, the Double-D stabilization problem has been solved. This compensator, r_{0A}, will be now used as the parameter in the Youla parametrization [12] with the initial compensator c_{0A} in order to get the final compensator for scenario A. This final compensator is

$$c_{fA} = \frac{x_{0A} + r_{0A} d_0}{y_{0A} - r_{0A} n_0} = \frac{4.594(s+1.786)(s+2.315)(s+1.596 \pm j2.044)}{(s+2.078)(s+8.938)(s+1.874 \pm j2.11)} \tag{11}$$

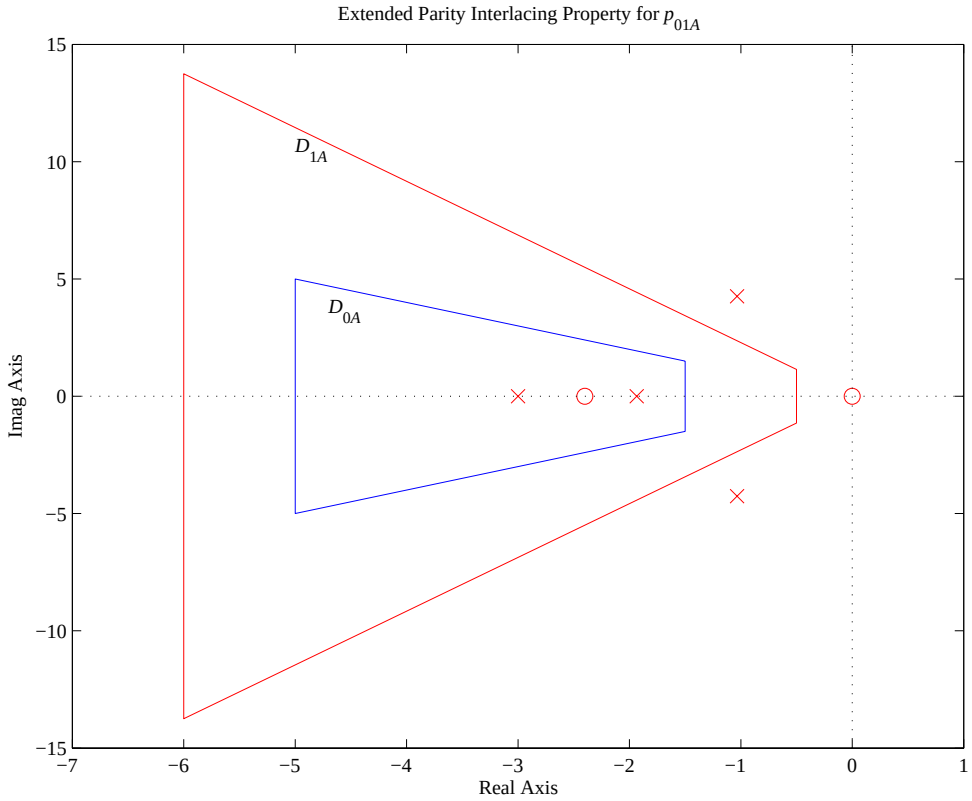

Fig. 3. Illustrating satisfaction of the Extended Parity Interlacing Property for associated system p_{01A}.

The final closed-loop poles for p_0 (blue) and p_1 (red) are seen in Fig. 5 to be in their respective stability regions. Thus, the design goals have been satisfied. The step responses of these compensated systems are shown in Fig. 6 and indicate stability for both systems. The performance of p_0 will be judged as acceptable for this example. We will assume that the overshoot for p_1 is larger than desirable even though the closed-loop poles are in the specified stability domain.

D. The Controller Design for Scenario B

The same procedure is used to design the final compensator for scenario B. First the associated system p_{01} is formed (actually, it should be called p_{10}), and a compensator that is stable with respect to D_{1B} is found to stabilize the associated system with respect to D_{0B}. The transfer function for the associated system is

$$p_{01B} = \frac{(d_1 n_0 - d_0 n_1)}{x_{1B} n_0 + y_{1B} d_0} = \frac{b_{01B}}{a_{01B}} = \frac{-b_{01A}}{a_{01B}} = \frac{-12s\,(s+2.4)}{(s+0.091)\,(s+3)\,(s+2.097 \pm j0.459)} \tag{12}$$

The coprime factorizations x_{1B} and y_{1B} are created in the same fashion as those in (8). The e.p.i.p. for p_{01B} is satisfied as shown in Fig. 7. The following compensator provides the stabilization with respect to D_{0B}.

$$r_{1B} = \frac{0.1996\,(s+2)\,(s+3.7)}{(s+1.65)\,(s+3.6)} \in S^{D_{1B}} \tag{13}$$

The {pole, zero} pair at $\{-3.6, -3.7\}$ is only used to produce a compensator as the same order as the one in Scenario A for simulation convenience during the reconfiguration part of the example; it is not needed to stabilize the associated system.

The closed-loop poles for (r_{1B}, p_{01B}), shown in Fig. 8 in blue, are seen to lie entirely in domain D_{0B}, and the compensator poles (shown in red) are seen to be in D_{1B}. Therefore, the Double-D stabilization problem for scenario B has been satisfied.

The parameter r_{1B} is used in the Youla parametrization with the initial c_{1B} compensator to obtain the final compensator for scenario B. This compensator is

$$c_{fB} = \frac{x_{1B} + r_{1B} d_1}{y_{1B} - r_{1B} n_1} = \frac{0.3045\,(s+2.079)\,(s+3.69)\,(s+0.839 \pm j0.31)}{(s+0.531)\,(s+2.028)\,(s+3.777)\,(s+4.199)} \tag{14}$$

The final closed-loop poles for p_0 (blue) and p_1 (red) are seen in Fig. 9 to be in their respective stability regions. The step responses of these compensated systems, shown in Fig. 10, indicate stability for both systems, and the performance of p_1 will

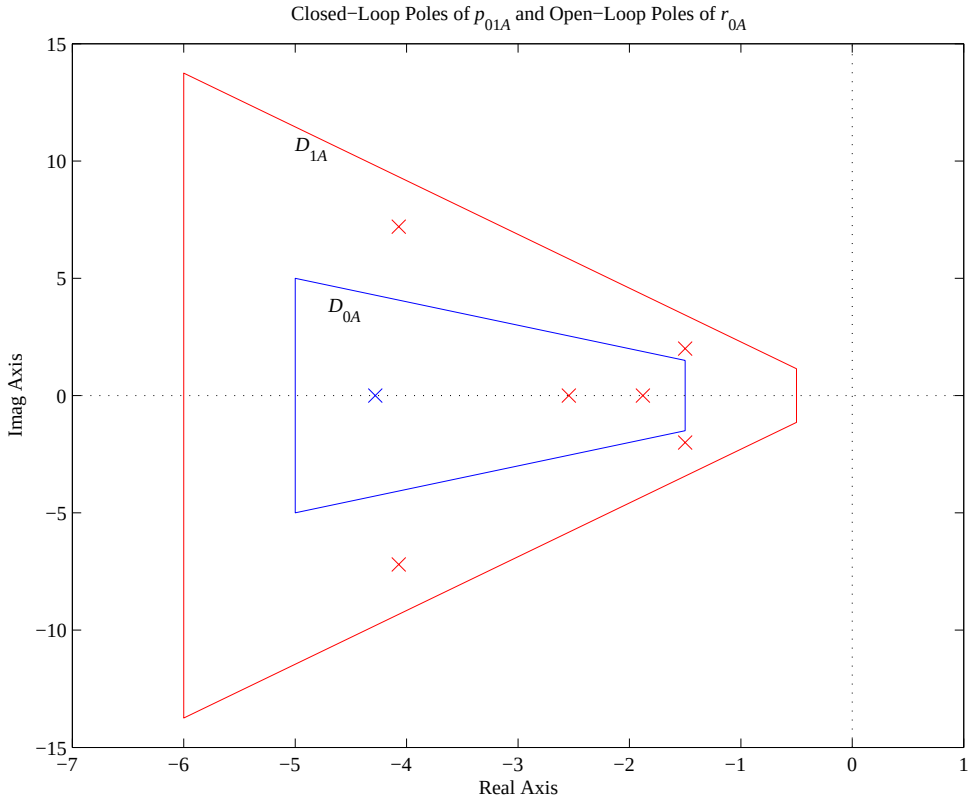

Fig. 4. Closed-loop poles of associated system p_{01A} and open-loop poles of its stable, stabilizing compensator r_{0A}.

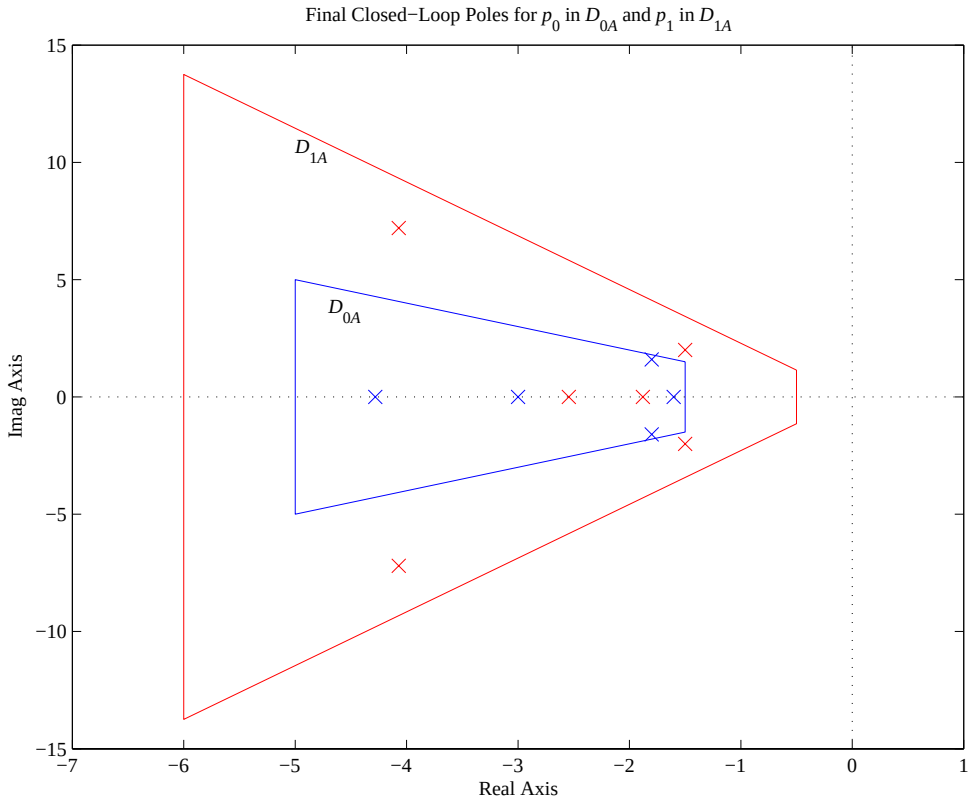

Fig. 5. Final closed-loop poles for $\{c_{fA}, p_0\}$ and $\{c_{fA}, p_1\}$ in their respective stability domains for Scenario A.

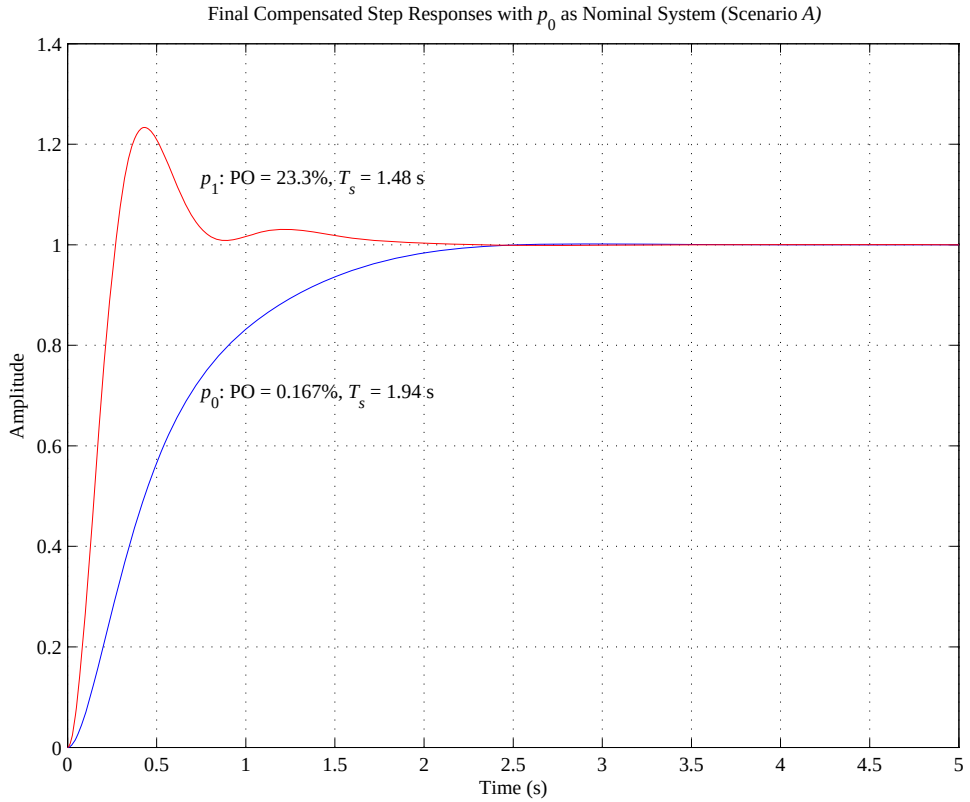

Fig. 6. Closed-loop step responses for $\{c_{fA}, p_0\}$ and $\{c_{fA}, p_1\}$ for Scenario A.

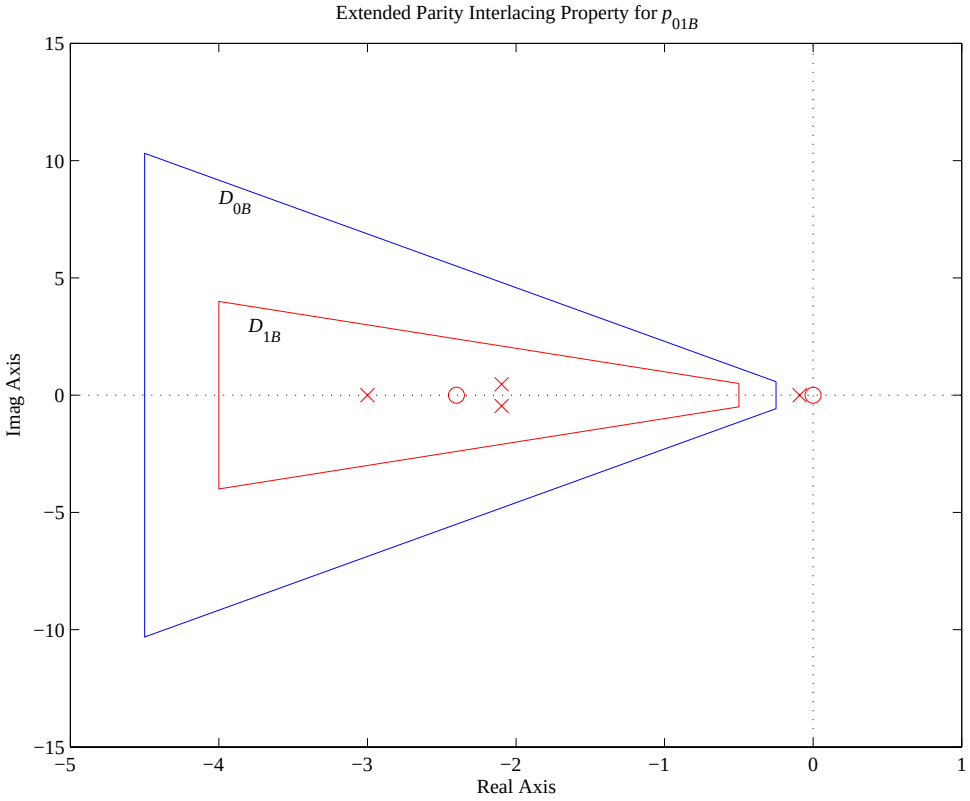

Fig. 7. Illustrating satisfaction of the Extended Parity Interlacing Property for associated system p_{01B}.

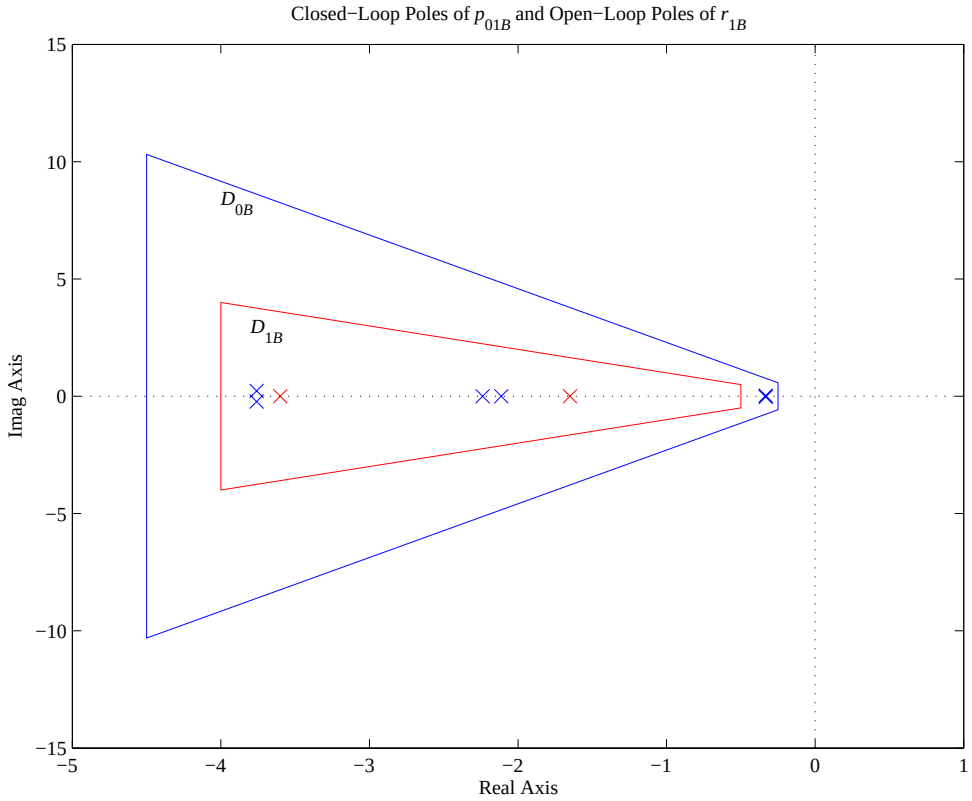

Fig. 8. Closed-loop poles of associated system p_{01B} and open-loop poles of its stable, stabilizing compensator r_{1B}.

be judged as acceptable for this example. Although the stability domain specifications have been satisfied, we will assume that the settling time for p_0 is longer than desirable.

Each of these two final compensators provides closed-loop stability for both system models and acceptable performance for the corresponding nominal model. In each case the compensator provides stability for the perturbed system even though performance is degraded. System identification or failure detection procedures may be used to determine which of the two models is correct at any point in time, and the appropriate compensator may then be selected. The simultaneous stabilization procedure yields a solution such that even if the wrong compensator is being used, closed-loop stability is maintained.

E. Reduced-Order Compensator

The final compensator in each of the scenarios is fourth-order. One criticism of simultaneous stabilization is the possibility of high-order compensators, particularly when there are three or more systems to be considered. Model reduction techniques can be investigated to possibly reduce the order of the final compensator without unduly sacrificing time domain or frequency domain results.

To determine how many states can be removed from the model, Hankel singular values can be computed. These singular values measure the relative energy in each of the states. Low-energy states can be removed without affecting performance[2]. The MATLAB® function *hankelsv.m* in the Robust Control Toolbox can be used for this. The Hankel singular values for the final compensator given in (14) for Scenario B are shown in Fig. 11. In can be seen that there is a drop of over two orders of magnitude in going from the second to the third singular value. Approximately 99.96% of the relative energy in this model is coming from the first two states, only 0.04% from the third and fourth states. Therefore, it is reasonable to reduce the order of the compensator from four to two. The function *reduce.m* can be used for this, resulting in the following reduced-order compensator.

$$c_{fB-reduced} = \frac{0.3045\,(s + 0.845 \pm j0.284)}{(s + 0.519)\,(s + 4.259)} \tag{15}$$

The step responses and the locations of the closed-loop poles are shown in Fig. 12. The step responses for both plants with both the fourth-order compensator in (14) and the reduced-order compensator in (15) are shown. It is clear that the reduced-order compensator has produced results that are indistinguishable from the fourth-order compensator. The closed-loop poles

[2]See the topic Hankel Singular Values in the MATLAB® Help file for the Robust Control Toolbox.

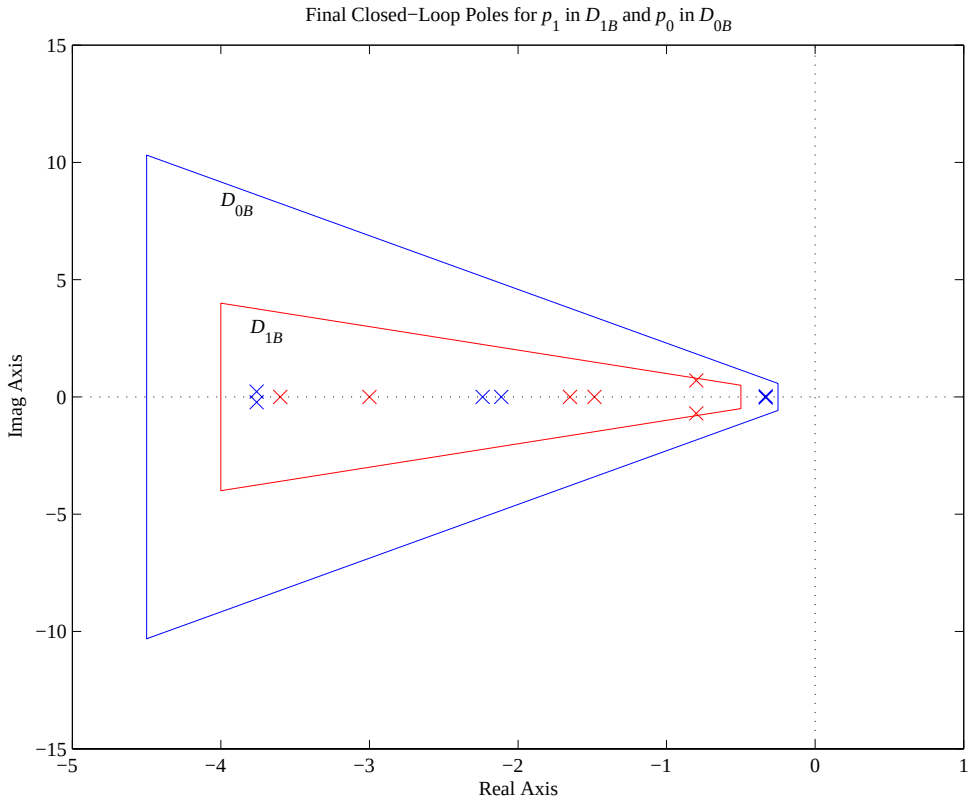

Fig. 9. Final closed-loop poles for $\{c_{fB}, p_0\}$ and $\{c_{fB}, p_1\}$ in their respective stability domains for Scenario B.

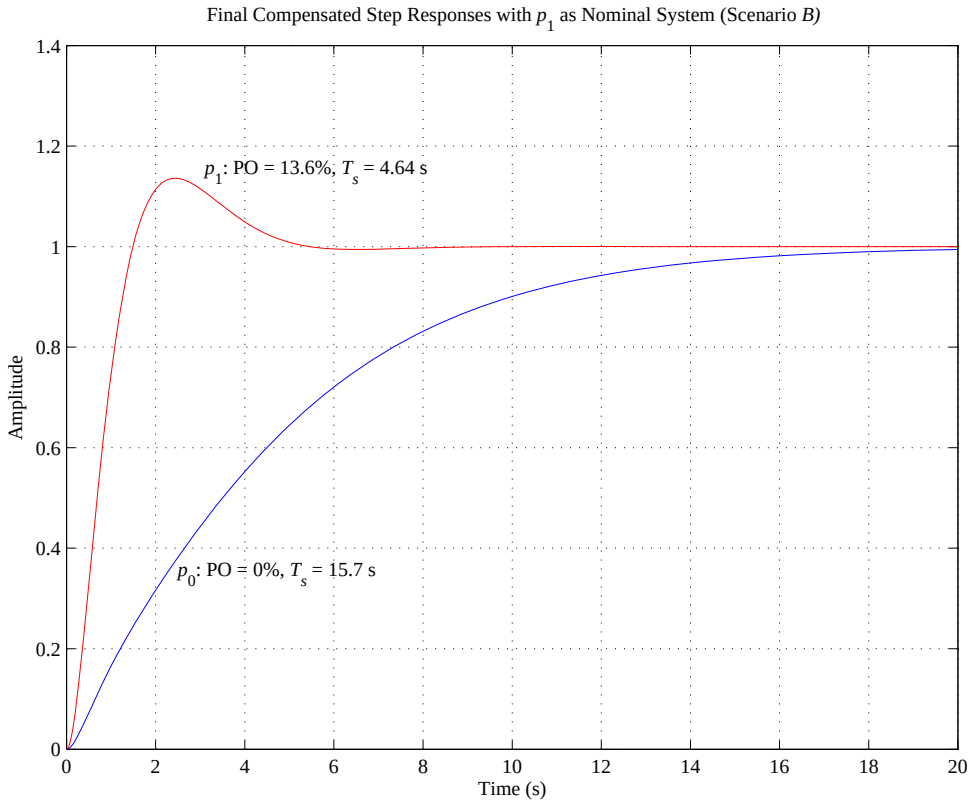

Fig. 10. Closed-loop step responses for $\{c_{fB}, p_0\}$ and $\{c_{fB}, p_1\}$ for Scenario B.

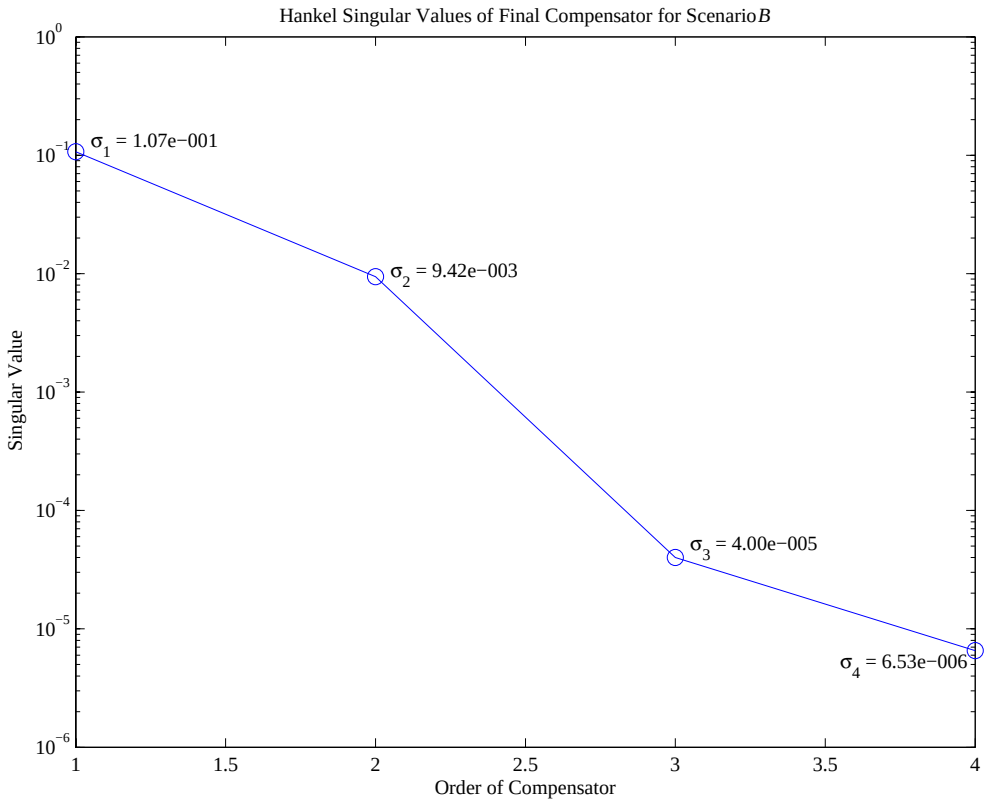

Fig. 11. Hankel singular values for the final compensator for Scenario B.

are seen to fall with their respective stability domains, so the original specifications also are still satisfied. Similar results are obtained when the fourth-order compensator in Scenario A is reduced to third-order. The step responses are virtually identical, and the closed-loop poles are all in their respective stability domains. However, if the order of the compensator is reduced to two for Scenario A, the closed-loop poles for the system with plant p_0 are all outside domain D_{0A} even though the step responses are nearly identical to those with the full-order compensator. Therefore, the third-order compensator of (16) must be used for Scenario A to satisfy the specifications, while the second-order compensator of (15) can be used for Scenario B.

$$c_{fA-reduced} = \frac{4.594\,(s+1.968)\,(s+1.591 \pm j2.094)}{(s+8.932)\,(s+1.845 \pm j2.167)} \tag{16}$$

F. Reconfigurable Control Simulation

To show the stability robustness of the controllers and the performance improvement that reconfiguration provides, a Simulink simulation was performed. The full-order controller and system model were in cascade with unity feedback. The reference input was a square wave of unit amplitude and a period of 12 seconds. The initial configuration was controller c_0 and plant p_0. Between 25 and 30 seconds, the plant was changed to p_1 through linear interpolation. This can represent a change in operating conditions or changes in component values. At 50 seconds, the controller was switched instantaneously to c_1, representing the result of failure detection or system identification. Between 75 and 80 seconds the plant was changed back to p_0 with linear interpolation, and at 99 seconds the controller was switched back to c_0. The block diagram for this simulation is shown in Fig. 13.

The results of this simulation are shown in Fig. 14. These switching times are not meant to model an actual situation. They do provide an illustration that closed-loop stability is maintained even when the incorrect controller is being used. Hopefully, the fault detection or system identification that would select the new controller would not take as long as was done in this simulation. The goal was to show a few cycles of the reference signal for each of the four {controller, plant} combinations. The simulation shows the obvious performance improvement that results when the correct controller is switched in. In the time response plot of Fig. 14, the vertical dotted lines indicate the beginnings of the transitions for the plants and the controller switching times. The current {controller, plant} pair is shown between the lines at the top of the figure. State space models were used to represent the plant and controller. The models were in observer canonical form so that the output signal would be continuous at the instant a switch in the plant model occurred.

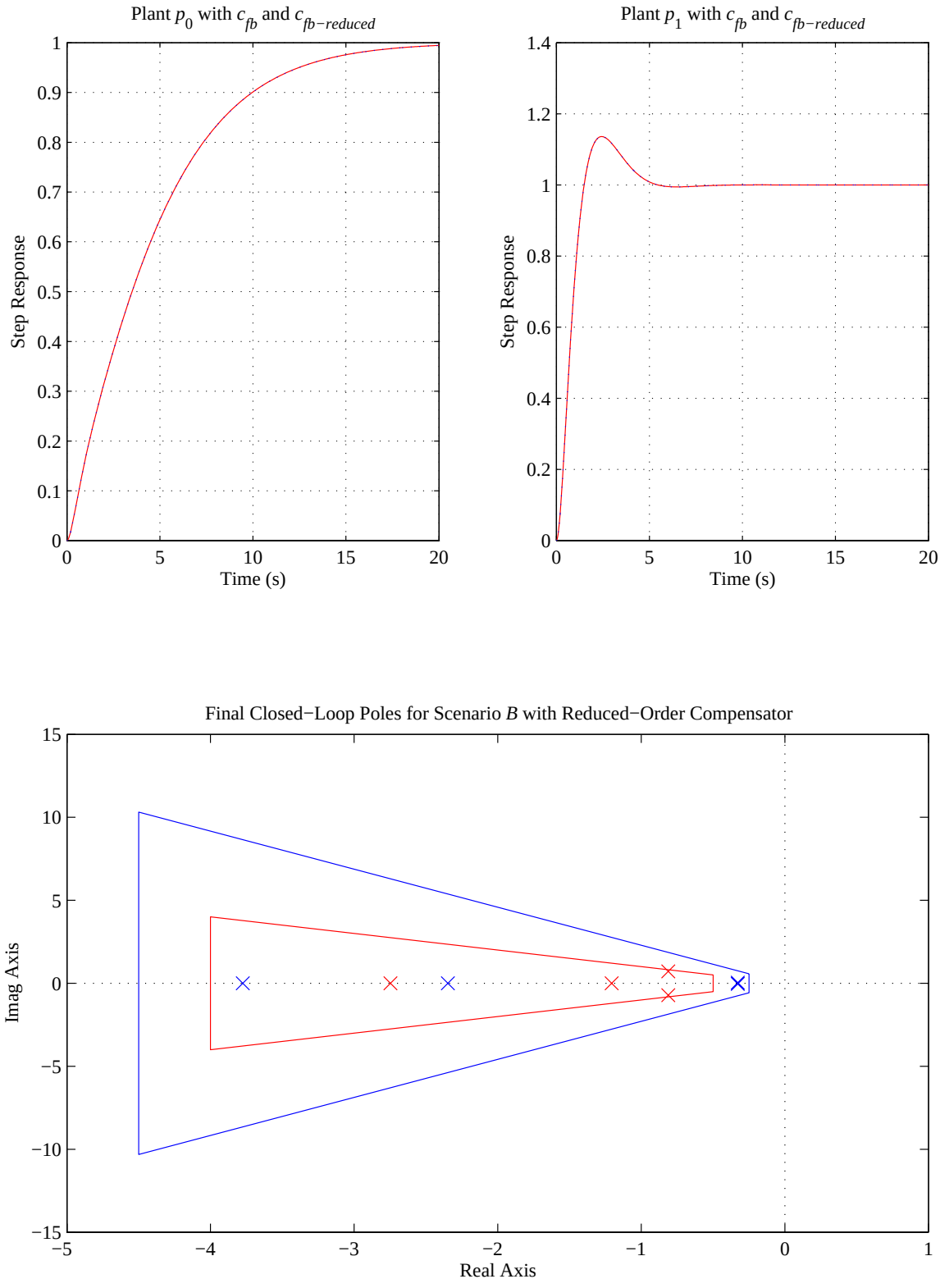

Fig. 12. Step responses and closed-loop pole locations for the reduced-order compensator for Scenario B.

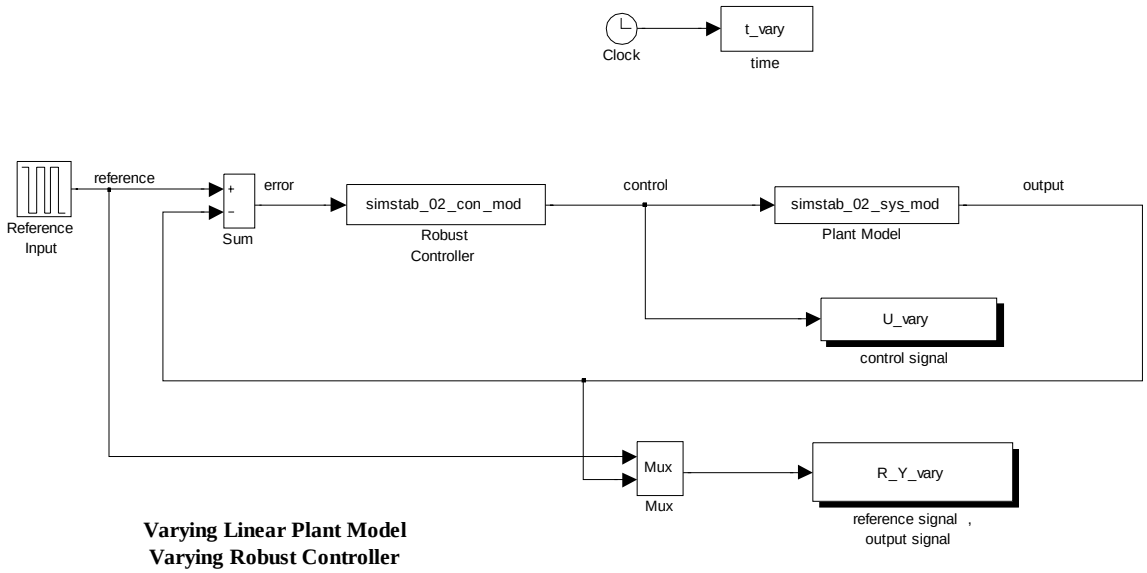

Fig. 13. Simulink block diagram for reconfiguration example.

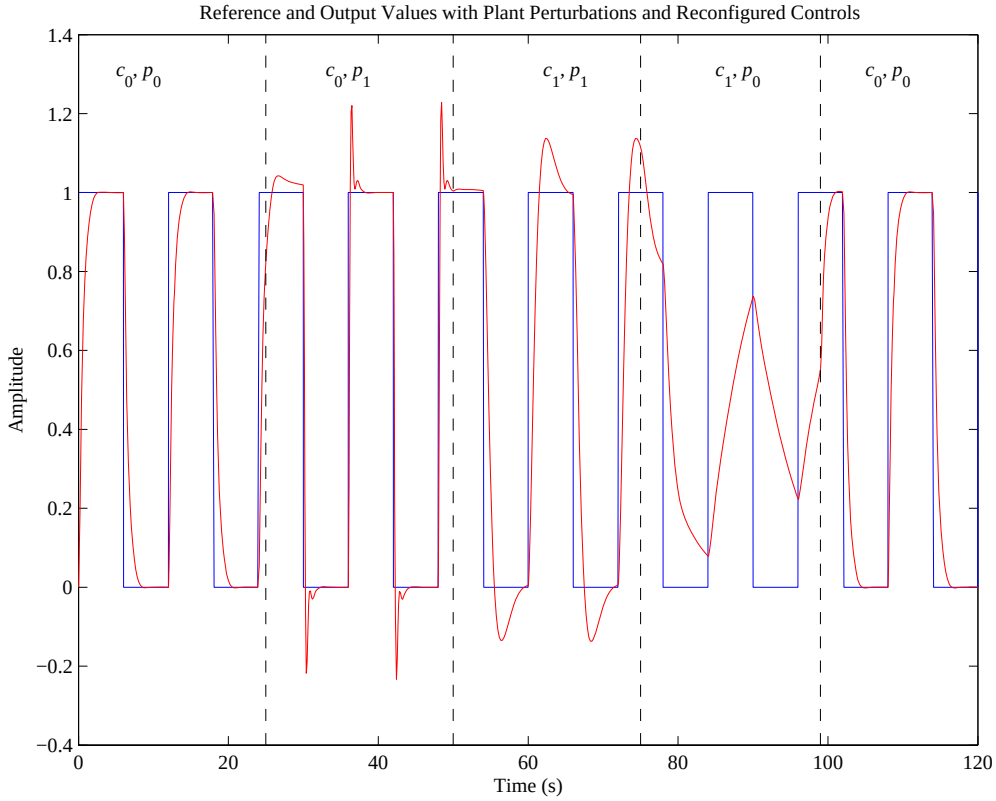

Fig. 14. Reconfiguration of the controllers in the face of plant perturbations.

REFERENCES

[1] M. Vidyasagar, *Control System Synthesis*. Cambridge, MA: MIT Press, 1985.

[2] E. S. Ammeen, *A New Simultaneous Stabilization Approach Using an Iterative Combining of System Models for the Design of Robust Control Algorithms*. PhD thesis, George Mason University, Jan. 1995.

[3] H. S. Kim, "A study in simultaneous stabilization for convex combinations of linear systems," Master's thesis, George Mason University, Aug. 1998.

[4] F. J. Arteaga-Bravo, *Simultaneous Stabilization with Multiple Bounded Domains of Stability*. PhD thesis, George Mason University, May 1995.

[5] F. Arteaga-Bravo and G. Beale, "Simultaneous stabilization with multiple bounded domains of stability in chemical process control," in *Proc. IEEE IECON 95*, (Orlando, FL), pp. 830–835, Nov. 1995. Orlando, FL.

[6] G. O. Beale and F. J. Arteaga, "Simultaneous stabilization with multiple bounded stability domains," *(KoREMA) Automatika*, vol. 37(1996) 3-4, pp. 91–98, May 1997.

[7] F. Arteaga-Bravo, G. Beale, and O. Montilla, "Multiple bounded domains for simultaneous stabilization: Interpolation conditions for two plants," in *Proc. Of SIAM Conference on Linear Algebra in Signals, Systems and Control*, (Boston, MA), April 2001.

[8] J. D. Gibson, *A Solution to the Double-D Stabilization Problem*. PhD thesis, George Mason University, May 1997.

[9] J. Gibson and G. Beale, "Convex parametrization for bounded domain stabilization," in *Proc. KoREMA 96*, (Opatija, HR), pp. 18–20, Sept. 1996.

[10] J. Gibson and G. Beale, "Stabilizing a nonlinear system over a range of operating points," in *Proc. 4th IFAC Conference on Maneuvering and Control of Marine Craft*, (Brijuni, HR), pp. 65–68, Sept. 1997.

[11] J. D. Gibson and G. O. Beale, "A geometric solution to the simultaneous bounded domain stabilization problem," *International Journal of Control*, vol. 73, no. 17, pp. 1536–1547, 2000.

[12] D. Youla, H. Jabr, and J. Bongiorno, "Modern wiener-hopf design of optimal controllers, part i: The scalar case," *IEEE Trans Auto Cont*, vol. AC-21, pp. 319–338, June 1976.